HHS Public Access

Author manuscript

Sci Signal. Author manuscript; available in PMC 2018 March 12.

Published in final edited form as:

Sci Signal. ; 10(484): . doi:10.1126/scisignal.aam5841.

The glycosylation pathway is required for the secretion of Slit and for the maintenance of the Slit receptor Robo on axons

Mary Ann Manavalan, **Vatsala Ruvini Jayasinghe**[1], **Rickinder Grewal**[2], and **Krishna Moorthi Bhat**[3]

Department of Neuroscience and Cell Biology, University of Texas Medical Branch School of Medicine, Galveston, TX 77555

Abstract

Slit proteins act as repulsive axon guidance cues by activating receptors of the Roundabout (Robo) family. During early neurogenesis in *Drosophila melanogaster*, Slit prevents the growth cones of longitudinal tract neurons from inappropriately crossing the midline, thus restricting these cells to trajectories parallel to the midline. Slit is expressed in midline glial cells, and Robo is present in longitudinal axon tracts and growth cones. We showed that the enzyme mummy (Mmy) controlled Slit-Robo signaling through mechanisms that affected both the ligand and the receptor. Mmy was required for the glycosylation of Slit, which was essential for Slit secretion. Mmy was also required for maintaining the abundance and spatial distribution of Robo through an indirect mechanism that was independent of Slit secretion. Moreover, secretion of Slit was required to maintain the fasciculation and position of longitudinal axon tracts, thus maintaining the hardwiring of the nervous system. Thus, Mmy is required for Slit secretion and for maintaining Robo abundance and distribution in the developing nervous system in *Drosophila*.

Keywords

Slit; Roundabout; axon guidance; Drosophila; Mummy; glycosylation

INTRODUCTION

The embryonic central nervous system (CNS) of the fruit fly *Drosophila melanogaster* consists of hemisegmentally reiterated units (hemineuromeres) containing similar sets of neurons and glia that extend along and on either side of the ventral midline in stereotypical patterns. Axons from these neurons run in tracts parallel to the midline and cross the midline at regular intervals to form commissures at two defined positions within each body segment,

[3]Corresponding author and contact: kmbhat@utmb.edu.

[1]Present address: Department of Cellular and Molecular Pharmacology, The Chicago Medical, School at Rosalind Franklin University of Medicine and Science, North Chicago, IL 60064

[2]Present address: Department of Medicine, University of Rochester Medical Center, 601, Elmwood Avenue, Rochester, NY 14642

Author contributions: K.M.B conceived the study. K.M.B., M.A.M., V.R.J., and R.G. contributed to the methodology. K.M.B., M.A.M., and V.R.J. performed data acquisition and analysis. K.M.B. performed revision experiments and revised the manuscript.

Competing interests: The authors declare that they have no competing interests.

Data and materials availability: All of the materials will be freely made available upon request.

giving the fly nerve cord a ladder like appearance. Axon tracts in the embryonic CNS of *Drosophila* can be roughly grouped into three types: (i) the longitudinal tracts, which run parallel to and on either side of the midline of the nerve cord but never cross the midline; (ii) the commissural tracts, in which axons cross the midline exactly once to connect the right and left hemineuromeres and become part of the longitudinal connectives together with longitudinal tracts; and (iii) the motor tracts, in which axons exit the nerve cord to innervate the musculature. The CNS also receives sensory tracts from the peripheral system. The paths of these tracts are strictly governed by several complementary guidance signaling systems (1–8), one of which is the Slit–Roundabout (Robo) system. In Slit-Robo signaling, the secreted ligand Slit binds to three different Robo proteins—Robo1, Robo2, and Robo3—to mediate growth cone repulsion (1–5, 8, 9). Controlling the pathfinding of axonal growth cones by Slit-Robo is remarkably conserved from flies to humans (8).

In the *Drosophila* embryo, Slit is produced only by the ventral midline glial cells (1–4) and interacts with Robo1, Robo2, and Robo3, which are present on growth cones and axons of the longitudinal tracts. Robo1 is also present in commissures but in very small amounts. The longitudinal tracts can be further subdivided into three main pathways: the medial (M) tract, which is closest to the midline; the lateral (L) tract, which is farthest from the midline; and the intermediate (I) tract, which is between the two (2, 3). Robo1 is present on axons of all three tracts, Robo2 is present in the L tract, and Robo3 is present in the I and L tracts (2, 3). When bound to Slit, these receptors initiate a signaling cascade that prevents the axons from inappropriately crossing the midline. Axons of the commissural tracts are able to cross the midline because the protein Commissureless (Comm) reduces the abundance of Robo on the surface of the commissures, thus allowing the growth cones to approach and cross the midline (10, 11). After crossing the midline, Robo is restored in these growth cones and axons, preventing them from crossing the midline again and allowing them to fasciculate with other axons of the longitudinal connectives.

A model to explain how Slit-Robo signaling guides different longitudinal axon tracts along the midline has been proposed (2, 3). In this model, Slit functions in a gradient. It is secreted from the midline, with the highest concentration at the midline. The concentration of Slit decreases with distance from the midline. This gradient of Slit activity mediates axon repulsion through Robo. In cultured cells, Slit appears to be secreted and deposited into the culture matrix (9). In embryos, Slit is detected only in the midline glia and in longitudinal axon tracts (4) but has not been reported to form an extracellular gradient. Thus, no direct proof exists that Slit is secreted in vivo. Signaling molecules that function as a gradient are often very sensitive to gene dosage effects (12), yet slit does not exhibit haploinsufficiency nor does duplication of *slit* cause axon guidance defects (1, 4). Moreover, overexpression of *slit* at the midline does not alter the positioning of axon tracts (1, 4), an essential feature of a gradient model. We previously showed that Slit from the midline glia is transported to the longitudinal connectives through commissural tracts (4). Robo1 is unlikely to be involved in transporting Slit because its abundance is low in commissural tracts in the midline region (10, 11) and Slit is transported to the connectives even in the absence of Robo1 (4). Robo2 and Robo3 appear to be absent in commissural tracts (2, 3), although one cannot entirely rule out the presence of low amounts of these two proteins in commissural tracts.

Finally, it is not clear how axon tracts are maintained after they are established and whether this is an active or a passive process. Although initial axon guidance is mediated by signaling pathways such as Slit-Robo, it is not clear whether Slit-Robo signaling is required for the maintenance of the position of tracts in the CNS. Here, we focused on the secretion of Slit, its interaction with Robo, and its role in axon tract maintenance using a mutation in *mummy* (*mmy*) (13), which encodes the only known uridine diphosphate–N–acetylglucosamine (UDPGlcNac) diphosphorylase in flies (14–16). This enzyme is involved in protein glycosylation, a posttranslational protein modification that is important for the proper trafficking and function of many secreted proteins (17, 18). Previous work has shown that loss of *mmy* causes defects in axon outgrowth and positioning, as well as defects in membrane localization of Wrapper, a protein involved in glial-axon interactions (15).

We found that Slit was glycosylated in an *mmy*-dependent manner and that glycosylation was essential for Slit secretion but not for binding to Robo1. Furthermore, loss of function for *mmy* reduced the abundance of Robo proteins in a manner that was independent of Slit. Finally, we show that Slit-Robo signaling was also essential for maintaining the position of axon tracts after pathfinding. These results provide new insight into several aspects of this important signaling system, including how Slit-Robo signaling might function in the absence of a Slit gradient.

RESULTS

Mummy is essential for axon guidance

We have previously shown that Slit is present not only in the midline glia but also in axon tracts (4). In a genetic screen using immunohistochemistry to identify mutations that perturb axonal architecture in *Drosophila* embryos, we identified one such mutation that we named *slim (slm)*. In *slm* mutants, axon bundles of the longitudinal connectives were narrower in comparison to wild type and inappropriately crossed the midline. The guidance defects in *slm* mutants were revealed by immunohistochemistry using antibodies recognizing Fasciclin II (Fas II), which stains longitudinal axon tracts (Fig. 1), and BP102, which stains commissural tracts (fig. S1). Fas II staining of wild-type embryos 9.5 hours post fertilization (hpf), which is during the early stages of axon tract formation, shows growth cones from the posterior corner cell (pCC), which pioneers the M tract (Fig. 1A). The I and L tracts are formed slightly later than the M tract, but all three tracts are visible with Fas II staining by 11 hpf (Fig. 1B). These neurons and their tracts are reiterated hemisegmentally along the nerve cord; thus, one half-segment is essentially the same as other half-segments. In *slm* embryos, the longitudinal tracts appeared normal at 9.5 and 11 hpf (Fig. 1, A and B, and Table 1). However, by 13 hpf, the longitudinal tracts showed major guidance defects: The M tract inappropriately crossed the midline, and the I and L tracts collapsed onto one another or onto the M tract (Fig. 1C). Furthermore, until about 11 hpf, the distances between these tracts in the *slm* mutant were approximately the same as in wild type, but by 13 hpf, the distance between the tracts and the midline and the distance between the tracts were greatly reduced (Fig. 1C and Table 1). Similarly, BP102 staining showed that the CNS in 10-hpf *slm* mutant embryos had normal commissural scaffolding. However, the commissures were thickened and closer to one another in older mutant embryos, suggesting that longitudinal

tracts are inappropriately crossing the midline (fig. S1). These defects were fully penetrant, with all *slm* mutant embryos showing these guidance defects.

Meiotic mapping and complementation analysis of the *slm* mutation using existing mutations and chromosomes that carry cytologically defined deletions (deficiency chromosomes) revealed *slm* to be an allele of *mmy*. Mutations in *mmy* were first isolated by Nüsslein-Volhard and colleagues in the 1980s (13), and previous studies have shown that *mmy* mutant embryos exhibit defects in dorsal closure, CNS fasciculation, and axon guidance (14, 15). We confirmed that *slm* is an allele of *mmy* by sequencing the *mmy* gene in *slm* mutants. The mutation in *slm* introduced a premature stop codon in *mmy* at amino acid position 75. This allele, hereafter referred to as mmy^{slm}, behaved as a genetic null because the axon guidance defects in mmy^{slm} were of the same strength and penetrance as in embryos homozygous for a deficiency of the *mmy* locus or in embryos transheterozygous for the deficiency and the *mmy*slm chromosome. Previous studies have shown that *mmy* encodes a UDP-GlcNac diphosphorylase (14, 15), which catalyzes the last step in the biosynthesis of UDP-GlcNac (16). UDP-GlcNac is one of the glycosyl donors for N- and O-linked glycosylation (14, 16). This enzyme is well conserved among eukaryotes, and *mmy* encodes the only UDP-GlcNac diphosphorylase enzyme in *Drosophila*.

Mummy is required for glycosylation of Slit

Because Mmy is an enzyme of the glycosylation pathway, we explored the possibility that it promotes axon guidance by regulating glycosylation of proteins involved in axon guidance. Given the similarity of axon guidance defects in *mmy* mutants to axon guidance defects in slit and robo mutants, we hypothesized that Slit might be glycosylated and that Mmy might regulate this modification. We performed Western blot analysis of extracts derived from 12- to 14-hpf wild-type embryos using two different antibodies recognizing Slit: a monoclonal antibody that recognizes the C terminus (Slit-C) (1, 9) and a polyclonal antibody that recognizes the N terminus (Slit-N) (4). Immunoblotting showed that full-length Slit had a molecular mass of 190 to 200 kDa (Fig. 2). This is higher than predicted based on the predicted mass of amino acid sequence of Slit (175 kDa), suggesting that Slit might be posttranslationally modified. We compared the molecular mass of Slit in extracts from 12- to 14-hpf wild-type, mmy^{slm}, and *mmy*1 embryos. Using the Slit-C and Slit-Nantibodies, we found that Slit from *mmy* mutants consistently migrated faster than Slit from wild-type embryos, with a molecular mass of 175 to 180 kDa (Fig. 2, A and B). This lower molecular mass is close to the calculated molecular mass of Slit based on its amino acid sequence. Furthermore, sequence analysis of Slit for putative N-linked glycosylation sites using a software that predicts glycosylation sites (NetNGlyc 1.0) (19) revealed that Slit contains 11 putative glycosylation sites, with 4 sites being particularly strong candidates for glycosylation (fig. S2).

To further confirm that Slit is glycosylated and that Mmy is involved in this modification, proteins extracted from 14-hpf wild-type embryos were treated with either a commercially available cocktail of enzymes that removes both *N*- and *O*-linked glycans or purified peptide-*N* glycosidase F (PNGase F), which removes only N-linked glycans. *N*-linked glycosylation involved the attachment of glycans to an asparagine, whereas *O*-liked

glycosylation is the addition of *N*-acetylgalactosamine to serine or threonine residues. We compared the molecular mass of Slit in treated versus untreated samples from wild-type embryos with the mass of Slit in extracts from *mmy* mutant embryos. Treating protein extracts from wild-type embryos with the glycosidase mix resulted in Slit migrating faster, with the same molecular mass as Slit from *mmy* mutant embryos (Fig. 2C). We also treated proteins extracted from 14-hpf wild-type embryos with PNGase F. This treatment also generated a faster-migrating Slit protein compared to the untreated sample (Fig. 2D). These results show that the Slit protein is N-glycosylated and that Mmy is essential for Slit glycosylation.

Zygotic loss of function of Mmy affects the glycosylation of Slit only during the latter part of neurogenesis

In *slit* mutants, axon guidance defects are seen early during the development of the CNS, as growth cones begin to extend, by 8 to 9 hpf (1). For example, a growth cone from the pCC neuron in ~9-hpf *slit* mutant embryo is tangentially projected toward the midline instead of along its normal trajectory, which is parallel to the midline (fig. S3A). However, in ~9-hpf *mmy* mutant embryos, the pCC projected normally (Fig. 1A). The absence of axon guidance defects in younger *mmy* mutant embryos is likely due to maternal deposition of the *mmy* gene products (mRNA or protein). Maternal deposition of transcripts and proteins direct the development of *Drosophila* embryos before activation of the zygotic genome and can compensate for some mutations that would otherwise affect zygotic development. This maternal effect often results in the rescue or partial rescue of zygotic defects. It has been reported that *mmy* transcripts are maternally deposited, and zygotic transcription of *mmy* begins only at ~7.5 hpf (20). Because mutations in *mmy* are homozygous lethal, it is not possible to generate embryos lacking maternally deposited *mmy* from *mmy*−/− females. In such cases of essential genes, the most common way to eliminate maternal deposition of a transcript of interest is to generate embryos from females with mosaic germ lines. However, germline *mmy* mutant clones are developmentally arrested and do not survive (20). Thus, it is not possible to examine axon guidance defects in embryos that lack both maternal and zygotic *mmy*.

Therefore, we took a functional approach to explore the lack of axon guidance defects in earlier stages of development in *mmy* mutant embryos. We hypothesized that maternally deposited Mmy may glycosylate Slit in early stages of development, thus masking the zygotic loss of function effect, but once the maternal store of Mmy is exhausted, it would result in the loss of Slit glycosylation and the onset of guidance defects. Because axon guidance defects in *mmy* mutant embryos initially become apparent by about 12 hpf, we reasoned that maternally derived Mmy should be exhausted by this time and not available to glycosylate Slit in ~12-hpf *mmy* zygotic null embryos. We examined the molecular mass of Slit by determining its mobility in extracts from 7- to 9-hpf wild-type and 12- to 14-hpf *mmy* mutant embryos. By Western blot analysis, the molecular mass of Slit in extracts from 7- to 9-hpfmutant embryos was the same as in wild-type embryos, indicating normal glycosylation of Slit at this time point (Fig. 2E). However, Slit had a lower molecular mass in12- to14-hpf *mmy* mutant embryos than in wild-type embryos of the same age (Fig. 2E). This indicates that Slit is not glycosylated in 12- to 14-hpf *mmy* mutant embryos. This age-

dependent change from glycosylated to nonglycosylated Slit corresponded with the age-dependent expressivity of axon guidance defects, allowing us to link axon guidance defects in *mmy* to the lack of glycosylation of Slit. These results also indicate that Slit signaling is essential not only for the initial guidance of growth cones but also later during neurogenesis to maintain the position of axon tracts it helped guide during early neurogenesis. Because the manifestation of axon guidance defects in *mmy* mutants correlates with the loss of Slit glycosylation, continual Slit signaling appears to be essential for maintaining the position of tracts within the nerve cord.

Mummy is essential for maintaining Robo in axon tracts

Because glycosylation is a common modification of cell surface proteins, we explored whether Robo1was also affected in *mmy* mutants. Western blot analysis of Robo1 in protein extracts from 7- to 9-hpfwild-type and 12- to 14-hpf mmy^{slm} embryos revealed that the molecular mass of Robo1 did not differ between mmy^{slm} and wild-type embryos at either time point (Fig. 3A). This suggests that Robo1 may not be glycosylated or heavily glycosylated. Because mobility assay is not sensitive enough to absolutely rule out glycosylation, Robo1 may still be a glycoprotein. However, as the following experiments show, Robo1 appears to be functional in mmy^{slm} mutant embryos, indicating that either Robo1 is not a glycoprotein or it can function even in the absence of glycosylation. Although the mobility of Robo1 was not affected in *mmy* mutants, we found that the abundance of Robo1 was reduced in 12- to 14-hpf *mmy* mutant embryos by as much as 75% but not in 7- to 9-hpfmutant embryos (Fig. 3A). These results show that Mmy is required for the maintenance of the abundance of Robo1 during neurogenesis. By quantitative polymerase chain reaction (qPCR) analysis, the abundance of robo1 transcripts in 12- to 14-hpf mmy^{slm} embryos (Fig. 3B) was reduced, but it was not statistically significant, suggesting that the difference was unlikely to account for the extent of reduction in the abundance of Robo1.

We also examined the spatial distribution of Robo1 in *mmy* mutant embryos by immunohistochemistry (Fig. 3C). In wild-type embryos, Robo1 is present in the M, I, and L tracts. In *mmy* mutant embryos, the domain of Robo1 distribution was narrower, suggesting that it is barely present in the M tract, much reduced in the I tract, and somewhat reduced in the L tract compared to wild type. This suggests that Mmy may control the spatial distribution of Robo1 across tracts. We also examined the abundance of Robo3 in *mmy* mutant embryos by immunohistochemistry because the antibody that recognizes Robo3 did not work well in Western blotting and the abundance of Robo2 by Western blot analysis because the antibody that recognizes Robo2 did not work well for immunohistochemistry. In wild-type embryos, Robo3 is present in the I and L tracts (Fig. 3D), as previously reported (2, 3), whereas in *mmy* mutant embryos, Robo3 was barely discernible in these tracts (Fig. 3D), suggesting that the abundance of Robo3 is also affected in *mmy* mutants. Robo2 is normally present only in the L tract. Western blot analysis of wild-type embryonic extracts with an antibody recognizing Robo2 showed a band at the molecular mass of ~200 kDa, which corresponded to the expected molecular mass for Robo2 (Fig. 3E). Another band at ~180 kDa was also observed (Fig. 3E), but it was also present in embryos homozygous for a deletion that removes both robo2 and robo3, indicating that it is a nonspecific background

band. Because we did not detect the ~200-kDa band in embryos deficient for robo2 and robo3, we conclude that it corresponds to Robo2. This band was also not detectable in *mmy*^{slm} embryos (Fig. 3E), suggesting that Robo2 was also reduced in *mmy* mutants. These results indicate that Mmy maintains the abundance and spatial distribution of all three Robo proteins.

It could be argued that reduced abundance of Robo proteins in *mmy*^{slm} is due to the lack of Slit that is available for binding. However, compared to wild-type embryos, the abundance of Robo1 was not reduced in embryos homozygous for a genetically null *slit* point mutation (*slit*^{2}) or a deficiency that removes *slit* (*slit*^{def}) (Fig. 4, A and B). On the other hand, the abundance of Robo1 was reduced in *slit*^{2} *mmy*^{slm} double mutants to the same extent as in *mmy*^{slm} single-mutant embryos (Fig. 4B). Thus, the decrease in the amount of Robo1 in *mmy*^{slm} was independent of *slit* but dependent on *mmy*. Therefore, reduction in the abundance of Robo in *mmy* mutants did not result from the lack or reduction of Slit. Mmy appears to maintain the abundance of Robo by an indirect, as yet unidentified, slit-independent mechanism.

Glycosylation of Slit is not essential for Slit binding to Robo1

We next sought to determine the molecular mechanism that underlies the axon guidance defects in *mmy* mutants. Several studies have shown that carbohydrate moieties on ligands are required for ligand-receptor binding in some contexts (21–24). To determine whether the nonglycosylated form of Slit that was present in *mmy* mutants was able to bind to Robo proteins, we performed Slit-Robo1 coimmunoprecipitation experiments in wild-type and *mmy* mutant embryos (Fig. 4C). We probed blots of Slit immunoprecipitates with the Robo1 antibody. The reciprocal experiment, probing Robo1 immunoprecipitates with the Slit antibody, was not performed because the Robo1 antibody did not work well for immunoprecipitation. Because the abundance of Robo1 was reduced in 12- to 14-hpf *mmy* mutants by as much as 75% (Figs. 3A and 4B), the amount of the total extract from *mmy* mutant embryos subjected to immunoprecipitation was increased by 75% compared to wild type. This was done to ensure that a comparable amount of Robo was available for immunoprecipitation in both the wild-type and *mmy* extracts. With similar amounts of Robo1 available for binding in wild-type and *mmy* extracts, nonglycosylated Slit in *mmy* was reproducibly able to bind to Robo1 (Fig. 4C). Robo1 did not coimmunoprecipitate with Slit in extracts derived from embryos deficient for *slit* (Fig. 4C). Thus, it seems unlikely that the loss of Slit signaling in *mmy* mutants results from the inability of Slit to bind to Robo proteins.

Pan-neuronal expression of robo1 does not rescue axon guidance defects in *mmy* mutants

It is possible that the axon guidance defects in *mmy* mutants are caused by the reduction in the abundance of Robo. To increase the abundance of Robo1, we expressed Robo1 pan-neuronally in *mmy*^{slm} embryos from a *UAS-robo1* transgene using the pan-neuronal driver *elav-GAL4*. Induction of the *UAS-robo1* transgene with elav-GAL4 increased the amount of Robo1 threefold, as indicated by Western blotting (Fig. 5A) and immunohistochemical analyses (Fig. 5, C and E). Pan-neuronal expression of Robo1 neither caused axon guidance defects in wild-type embryos nor rescued the axon guidance defects in *mmy*^{slm} embryos

(Fig. 5, C and E). One could argue that the lack of rescue was due to the overexpression of only Robo1 and that, for rescue, it is essential to restore the abundance of all three Robo proteins. However, only Robo1 is present in the M tract, whereas Robo2 and Robo3 are restricted to the L and I tracts (2, 3), and the M tracts are largely unaffected in *robo2 robo3* double mutants (fig. S3B). Because the overexpression of Robo1 did not rescue the M tract defect in mmy^{slm}, we conclude that the observed axonal tract defects in *mmy* mutants are due to the loss of Slit function and upstream of the defect in the abundance of Robo proteins.

Mmy-dependent glycosylation of Slit is required for Slit secretion

Because glycosylation is important for sorting proteins into the secretory pathway (17, 18), it is possible that Slit might not be secreted in *mmy* mutants and thus unavailable for interaction with Robo. Although *slit* is transcribed exclusively in the midline glial cells, Slit protein is present not only in the midline glia but also in the commissural and longitudinal axon tracts (4, 25). In wild-type embryos, Slit is most abundant in axon tracts where they cross the midline (in the commissural tracts) adjacent to the Slit-expressing midline cells (Fig. 6, A to C). Slit appears to be transported or diffused along the commissural tracts where they cross the midline. This observation is consistent with the finding that the loss of commissures in *comm* mutants greatly reduces or eliminates the Slit protein in axonal tracts (4).

We reasoned that the presence of Slit in the axon tracts could be used as an indicator for Slit secretion from the midline, allowing us to determine whether the loss of Slit glycosylation in *mmy* mutants affects Slit secretion. In mmy^{slm} embryos, Slit was restricted to the midline cells and absent in the commissural and longitudinal tracts (Fig. 6). We observed the reduction of Slit in axonal tracts using the diaminobenzidine (DAB) peroxidase and the more sensitive alkaline phosphatase (AP) immunohistochemical detection procedures (Fig. 6, A and B), as well as by fluorescent confocal imaging of Slit (Fig. 6C). No Slit was detected in the axon tracts of mmy^{slm} embryos with any of these three methods (Fig. 6, A to C). Thus, while in wild-type embryos, Slit was present in the midline glial cells, commissural tracts, and longitudinal tracts, in mmy^{slm} embryos, Slit was restricted to the slit-expressing midline glial cells and was not observed outside of these cells (Fig. 6). This difference in the pattern of Slit localization in the ventral nerve cord between wild type and *mmy* mutants was clearly seen with ImageJ analysis of the Slit profile across CNS (Fig. 6, D and E). Slit protein localization in *mmy* mutant embryos resembled that of slit RNA in wild type, as shown by histochemical (Fig. 6F) and ImageJ analysis (Fig. 6G). These results indicate that Slit is not secreted from the midline glial cells in mmy^{slm} embryos.

To confirm that Mmy-dependent glycosylation of Slit is essential for Slit secretion, we analyzed the distribution of intracellular and extracellular Slit by modifying the embryo culture method of Perrimon and colleagues (26). We dissociated wild-type and mmy^{slm} embryos in culture medium, but instead of culturing the cells, we immediately tested for the presence or absence of Slit in both the medium and in the cells. Glycosylated Slit was present in both the medium and the cells in 11- to 12-hpf wild-type embryos but present only in the cells in mmy^{slm} embryos (Fig. 7). The absence of tubulin in the medium fraction indicated that this procedure did not cause cell lysis. These results show that glycosylation

of Slit depends on Mmy, which is essential for Slit secretion. We detected glycosylated Slit in the medium of both wild-type and *mmy*^{slm} embryos at 5 to 6hpf (fig. S4), consistent with the perdurance of maternally contributed Mmy until at least 11 hpf.

To determine whether Mmy function in only the midline glial cells was sufficient for the secretion of Slit, we transgenically expressed a wild-type *mmy* transgene in midline glia of *mmy*^{slm} mutants using the midline driver *sim-GAL4*. Expression of *mmy* in midline cells restored Slit in the axon tracts (Fig. 8A) and partially rescued the axon guidance defects (Fig. 8B). This partial rescue suggests that Robo proteins in *mmy* mutants were functional. It is likely that the rescue of the axon guidance defects was not complete because the expression of *mmy* in the midline cells alone did not restore the abundance of Robo1 in the axons (Fig. 8C). Consistent with this possibility, expression of *mmy* in both neurons and midline glia in *mmy*^{slm} mutants rescued Slit secretion (Fig. 8D), axonal guidance defects (Fig. 8E and Table 2), and Robo1 abundance (Fig. 8F).

DISCUSSION

The Slit protein is a major axon guidance cue across species (1–9). We show that Slit is glycosylated in an Mmy-dependent manner and that glycosylation of Slit is essential for its secretion. We also found that Slit-Robo signaling is likely required after the initial pathfinding period for maintaining the position of the axon tracts within the nerve cord. In the absence of a continual Slit-Robo signaling, tracts defasciculate and shift toward the midline. Other guidance molecules might also be essential for axon maintenance. Furthermore, this study also reveals that there is a glycosylation-dependent mechanism that maintains the abundance and spatial distribution of Robo proteins. Our data also suggest a mechanism by which Slit-Robo signaling can control early and late CNS development without the need to invoke a concentration-dependent response to Slit.

Previous work on Slit showed that Slit is recovered from the culture medium of cells expressing a *slit* transgene (9). It has been proposed that Slit is secreted from the midline glia in vivo, forming a gradient that extends outward from the midline (1–3). Although a gradient of Slit has not been demonstrated and overexpression of Slit in the midline has not been shown to alter the position of the axon tracts, Slit is present beyond the midline in axon tracts (1, 4, 9, 25). Slit is secreted from the midline glial cells in vivo, but it is distributed specifically along the axon tracts and not throughout the neurectodermin the form of a gradient. We do not know how Slit is transported along the axonal tracts. Slit could be internalized, transported intracellularly, and secreted again to enable it to interact with Robo. Alternatively, Slit could be transported along the commissural axonal tracts by binding to extracellular matrix proteins or diffusing along the tracts.

Our results shed light on short- and long-range Slit signaling and how Slit-Robo might regulate both the initial growth cone guidance and the subsequent maintenance of the position of axon tracts within the nerve cord. During the initial growth cone guidance phase (7 to 11 hpf), the Robo-expressing growth cones extend toward the midline where they encounter Slit. Interaction between Robo and Slit makes the growth cones turn away from the midline. The distribution pattern of the three Robo receptors in growth cones should

create a functional gradient for Robo. That is, growth cones of the M tract have only Robo1, those of the I tract have Robo1 and Robo3, and those of the L tract have Robo1, Robo2, and Robo3 (2, 3). Thus, the combined highest concentration of Robo proteins would be in the L tract, followed by the I tract, and the least in the M tract (only Robo1). This could create a situation similar to having a gradient of Robo, resulting in the differential positioning of the three tracts: The L tract moves farthest from the midline, and the M tract moves closer to the midline, with the I tract positioning in between. Thus, we think that it is the distribution of Robo and not a Slit gradient that defines the initial position of the tracts relative to the midline. Previous results showing that overexpression of *robo2 or robo3* shifts axon tracts further away from the midline (2, 3, 27) are consistent with this possibility.

Slit that reaches the longitudinal connectives either spreads within the longitudinal connectives or remains bound to the extracellular matrix of the commissural tracts and interacts with Robo receptors in longitudinal tracts. A local interaction between Robo and Slit would then mediate the maintenance of spacing between the tracts and between the tracts and the midline. This is consistent with the fact that in *mmy* mutants where Slit is not in the tracts, the longitudinal tracts defasciculate and move closer to the midline. Physical constraints in these older embryos may prevent these tracts from completely collapsing at the midline. In addition, in *mmy* mutant embryos, the distance between the M, I, and L tracts decreases as well (Fig. 1 and Table 1), which is likely due to the loss of Slit from these tracts. Further support is provided by the fact that although midline expression of *mmy* in *mmy* mutant embryos restored Slit secretion and partially rescued axon guidance defects, there was still a loss of spacing between the longitudinal tracts (Fig. 8B and Table 2). Reduced interactions between Robo and Slit in the tracts in these rescued embryos are likely the cause for the spacing defects. It is reasonable to propose that Mmy is necessary for secretion of Slit because only the glycosylated form of Slit is properly trafficked inside cells. However, we cannot, at this point, formally rule out the possibility that Mmy modifies other proteins that are involved in the intracellular trafficking of Slit or the transport of Slit from midline cells to axon tracts. Mmy is the only known UDP-GlcNac diphosphorylase in *Drosophila*, so it is almost certainly involved in the glycosylation of other proteins that play a role in neuronal pathfinding and adhesion such as the heparan sulfate proteoglycan (HSPG) syndecan. HSPGs serve as cell adhesion regulatory and signaling molecules (co-receptors) (28, 29) and appear to be involved in the regulation of Slit-Robo signaling not only in *Drosophila* but also in other organisms such as *Caenorhabditis elegans* and zebrafish (29–33). It has been reported that syndecan binds to and stabilizes Slit-Robo complexes (29, 33, 34). Loss of Mmy activity could therefore indirectly affect Slit-Robo signaling through syndecan. Because Slit is not secreted in *mmy* mutants, temperature sensitive alleles of *mmy* would be required to test whether Mmy affects syndecan's ability to promote Slit-Robo signaling.

With respect to Robo proteins, Mmy likely affects their abundance indirectly. Given our qPCR results for *robo1* in *mmy* mutants, we think that it is unlikely that Mmy affects the transcription of robo genes. Robo proteins might also be glycosylated; however, our gel mobility assay did not indicate that they are (Fig. 3A). Although heavily glycosylated proteins will exhibit shifts in mobility, gel mobility assays are not sensitive enough to detect small amounts of glycosylation. Therefore, it is still possible that Mmy is required for

glycosylation of Robo, which could in turn affect the folding or trafficking of Robo. However, the Robo proteins present in *mmy* mutants appear to localize to axons just as they do in wild type (Fig. 3). Even if Robo proteins are not properly distributed on the membrane, that alone is unlikely to cause a reduction in the abundance of Robo. For example, the glial cell surface protein Wrapper is not properly localized in *mmy* mutants, yet there is no accompanying reduction in the abundance of Wrapper (15). The Robo proteins that are present in *mmy* mutants appear to be functional as well because midline expression of *UAS-mmy* in *mmy* mutants partially rescued the axon guidance defects (Fig. 8B). Therefore, the simplest explanation would be that Mmy modifies other proteins, presumably by glycosylation or glycosylphosphatidylinisotol anchoring, that stabilizes Robo. However, we do not exclude the possibility that the effect of loss of function for *mmy* on Robo proteins could be a combination of lack of a putative glycosylation, improper distribution on the membrane, and degradation. Regardless, the effect of Mmy on Robo is separate from and downstream of its effect on Slit.

Because Mmy is the only UDP-GlcNac diphosphorylase in *Drosophila*, it is likely required for all N-linked glycosylation events. It is also likely that some proteins may be more sensitive than others to loss of *mmy* activity, perhaps depending on the extent of their glycosylation. For example, Fas II is a glycoprotein, yet it appears to be normally present in zygotic null late-stage *mmy* mutant embryos. Thus, not all glycoproteins are similarly affected in *mmy* zygotic mutants. It may depend on many factors, such as protein abundance and the cell type in which the protein is produced. Maternal *mmy* may be depleted at different rates in different cell types as well. Moreover, protein turnover rate may also play a role, with the longest-lived proteins being the least affected by the zygotic loss of *mmy*.

Slit-Robo signaling and axon guidance are intensely studied. However, emphasis in the field has always been on understanding the events controlling the initial process of axon guidance. Here, we show that Slit-Robo signaling is required not only at the initial stages of axon guidance but also later for maintaining the position of the axon tracts. This maintenance function of Slit-Robo signaling appears to prevent defasciculation and inappropriate midline crossing by individual axon tracts within the bundle or shifting of the position of axons toward the midline. One could argue that the tracts that cross the midline in older *mmy* mutant embryos originate from late-forming neurons when maternal Mmy is exhausted. However, the reduction in the spacing between the entire tracts and across the midline in older-stage embryos (see Fig. 1C and Table 1) argues that functional Slit is continuously needed to maintain the correct spacing between the tracts. Thus, our results argue that axon guidance signaling systems are required for tract homeostasis throughout the lifespan.

MATERIALS AND METHODS

Fly stocks and genetics

Standard fly rearing and genetics procedures were used (35). The mmy^{slm} mutation was identified as a background mutation associated with a deficiency chromosome [Bloomington *Drosophila* Stock Center 6067: Df (2L) fn7, pr1 cn1/CyO, P{GAL4-twi.G}2.2, P{UAS-2xEGFP} AH2.2], in an immunohistochemistry-based screen for mutations that

cause a loss of Slit protein from the axon tracts and show axon guidance defects. We recombined the *mmy*^{slm} mutation away from the deficiency to recover *slm* and deposited the *slm*-free deficiency chromosome in the Bloomington *Drosophila* Stock Center. The following mutant and transgenic strains were obtained from the Bloomington *Drosophila* Stock Center: *mmy1*, *mmy*^{def} [Df (2L) BSC6, dp (ov1) cn1/SM6a; BL# 6338], *slit*^{2}, *slit*^{def} [w[118];Df (2R) JP5/CyO, P{sevRas1.V12} FK1; BL# 3519], *robo1*^{4}, *robo1*^{def} [w[118];Df (2R) BSC786/SM6a; 58F4- 59B1; BL# 27358], *robo2, robo3*^{def} (which uncovers both the *robo2* and *robo3* genes [w[118]; Df (2L) ED108, P{3′.RS5+3.3′}ED108, P{3′.RS5+ 3.3′}ED108/SM6a; BL# 24629]), *sim-GAL4* (on the third chromosome), *slit-GAL4* (on the second chromosome), and *elav-GAL4* (on the X chromosome). The following mutant and transgenic strains were obtained from C. Goodman: *slit*$^{E\text{-}158}$ (*slit*^{hypo}, a P-element insertion allele) and *UAS-robo1* (X chromosome insertion). We generated the *UAS-mmy* transgenic line (on the X chromosome). We generated the *slit*^{2} *mmy*^{slm} double mutants and *mmy*^{slm} *slit-GAL4* line by meiotic recombination. The recombinant *slit*^{2} *mmy*^{slm} chromosome was confirmed by complementation analysis with *robo4* and a deficiency that uncovers both *robo2* and *robo3* [w^{1118}; Df (2L) ED105, {w[+mW.Scer \FRT.hs3]=3′.RS5+3.3′}ED105/SM6a; BL# 24118]. For *robo2 robo3* double-mutant analysis, we used Df (2L) ED108, which removes both these genes. Chromosomes were balanced using green fluorescent protein (GFP)–marked balancers to enable the selection of homozygous mutant embryos. Mutant embryos were further identified using phenotypes in other tissues and lineages.

Mapping of *mmy*^{slm} and identifying the molecular lesion

The *slm* mutation was initially mapped to the second chromosome by using marked balancer chromosomes and monitoring the segregation of the mutation. The precise location was determined by complementation analysis with overlapping deficiencies on the second chromosome and with the known alleles from within the smallest deficiency that failed to complement *slm*. We identified molecular lesion in the *mmy* gene in *slm* mutation by sequencing the gene, as described previously (4). Briefly, DNA was extracted from about 100 *mmy* mutant embryos and subjected to PCR using six different sets of *mmy*-specific primers to amplify short segments of the DNA across the *mmy* gene in the *mmy*^{slm} mutant chromosome. The DNA was then sequenced at the University of Texas Medical Branch (UTMB) DNA sequencing core facility, and the mutational change was identified by sequence alignment with the wild-type gene.

Generation of *UAS-mmy* transgenic line and rescue experiments

To generate *UAS-mmy* transgenic line, a full-length *mmy* complementary DNA (cDNA) was obtained from the *Drosophila* Genomics Resource Center and cloned into the UAS transformation vector (36). The cDNA was sequenced before and after cloning into the transformation vector to check sequence integrity. This *UAS-mmy* construct was used to generate transgenic lines at GenetiVision, a *Drosophila* transgenic service company. To determine whether *UAS-robo1* could rescue *mmy* mutant phenotypes, *UAS-mmy* was introduced to an *mmy* mutant background, and the transgene was induced using the *elav-GAL4* driver at 29°C. The embryos were then examined for Robo1 by Western blot and immunohistochemistry analyses and for the rescue of the axon guidance defects. To

determine whether the expression of *mmy* in the midline in *mmy* mutants restores secretion of Slit and rescues axon guidance defects, *UAS-mmy* was introduced to the mmy^{slm} mutant background and induced in the midline glia using *sim-GAL4* at 29°C. The embryos were then examined for the distribution of Slit and Robo, as well as for the rescue of the axon guidance defects. To determine whether the expression of *mmy* in the midline as well as in neurons in *mmy* mutant background restores secretion of Slit and rescues axon guidance defects, mmy^{slm} was recombined with the *slit-GAL4* chromosome and then introduced to the *UAS-mmy* and *elav-GAL4* backgrounds and induced in the midline glia using *slit-GAL4* and in neurons with *elav-GAL4* at 29°C. The embryos were then examined for the distribution of Slit and Robo, as well as the rescue of the axon guidance defects.

Immunohistochemistry and microscopy

Immunochemistry was carried out as described previously (4, 25, 37). Monoclonal antibodies recognizing the following proteins were used at the indicated concentrations: Fas II [1:20, mouse monoclonal 1D4; Developmental Studies Hybridoma Bank (DSHB)], Slit-C (1:20, mouse, C555.6D; DHSB), Robo1 (1:3, mouse, 13C9; DHSB), and Robo3 (1:3, mouse, 14C9; DHSB). The monoclonal antibody BP102, which recognizes an unknown epitope on *Drosophila* axons, was used at 1:4 (AB_528099; DHSB). For confocal microscopy, secondary antibodies conjugated to Cy5 (rabbit, 1:400, A10523; Invitrogen), fluorescein isothiocyanate (mouse, 1:50, 62–6511; Invitrogen), Alexa Fluor 488 (rabbit or mouse, 1:300, A-11008 or A-11001; Invitrogen), or Alexa Fluor 647 (rabbit or mouse, 1:300, A-21245 or A-21236; Invitrogen) were used. For light microscopy, secondary antibodies conjugated to alkaline phosphatase (rabbit, 1:200, 31341; Pierce) or horseradish peroxidase (HRP) (rabbit, 1:200, 31460; Pierce) were used. Alkaline phosphatase was detected using 5-bromo-4-chloro-3-indolyl phosphate and nitro blue tetrazolium (S3771; Promega). HRP was detected with DAB (D4418; Sigma-Aldrich). Whole-mount RNA in situ hybridization for *slit* was done as described previously (21) using a digoxigenin-labeled *slit* probe synthesized by PCR (21), and the color reaction was developed by AP reaction. With the DAB color reaction, the staining develops within 3 to 5 min and only marginally darkens with time; with AP, the staining progressively gets darker with time. In all our immunostaining procedures, the control or wild-type embryos and mutant embryos were from the same collection plates and processed in the same tube so that there was no difference in the staining time or conditions. Various genotypes were identified using appropriate markers and phenotypes.

Western blot analysis

Western blot analysis was done as described previously (4, 21). About 30 embryos of the specified age were collected and used for protein extraction, as follows. Embryos were collected on egg-laying plates, transferred to a small mesh-wire basket, and washed with running water, and the mutant embryos were selected (absence of green excitation for GFP) using an ultraviolet (UV) light–equipped Zeiss microscope. The embryos were lysed in 40 μl of extraction buffer [0.15 M NaCl, 0.02 M tris (pH 7.5), 0.001 M EDTA, 0.001 M $MgCl_2$, 1%Triton X-100, and protease inhibitor cocktail (PIC)]. The lysis was done by sonication for 1 min on ice in a 1.5-ml Eppendorf vial using a handheld sonicator (Thermo Fisher Scientific) equipped with a disposable pestle (Thermo Fisher Scientific). The lysates were

centrifuged for 5 min at 13,000 rpm in a microfuge (Beckman). The supernatant was collected and, 10 μl of 4× Laemelli buffer and 1.5 μl of the reducing agent (Invitrogen) were added, boiled in water for 10 min, and cooled on ice. About 15 embryos (equivalent amounts of each extract) were loaded per lane on a 4 to 12% premade SDS–polyacrylamide gel electrophoresis (PAGE) gels (Invitrogen). Two different primary antibodies recognizing Slit were used: Slit-N, which recognizes the N-terminal portion (1: 50000) (4), and Slit-C, which recognizes the C-terminal portion (mouse, C555.6D, 1:100; DHSB) (1, 9). For Robo1 Western blotting, mouse monoclonal 13C9 (DHSB) was used at 1:40 (25), and for Robo2 Western blotting, a rabbit polyclonal antibody (3) was used at 1:100. Signals were detected by the chemiluminescent reaction kit (Millipore). The chemiluminescence signal was quantified using the AlphaEaseFC software (21). An antibody against tubulin (1:4000; Abcam) was used to reprobe the blots to determine the loading control.

Glycosidase assays

Two different glycosidases were used to investigate the glycosylation of Slit: protein deglycosylationmix (P6039S; New England Biolabs), which consists of PNGase F, *O*-glycosidase, neuraminidase, β1–4 galactosidase, and β-*N*-acetylglucosaminidase and removes both *N*- and *O*-linked oligosaccharides from glycoproteins, and PNGase F (P0704S; New England Biolabs), which specifically removes N-linked oligosaccharides. About 30 wild-type and homozygous mutant embryos were selected and aged until 12–14 hpf. The homozygous mutant embryos were selected under the UV microscope based on GFP. These embryos were lysed in 40 μl of extraction buffer [0.15 M NaCl, 0.02 M tris (pH 7.5), 0.001 M EDTA, 0.001 M MgCl2, 1% Triton X-100, and PIC] on ice for 15 min. The lysates were centrifuged for 5 min at 13,000 rpm. For deglycosylation, 18 μl of the supernatant was mixed with 2 μl of 10× glycoprotein denaturing buffer (0.5% SDS, 40 mM dithiothreitol), and this reaction mixture was denatured by heating at 100°C for 10 min, followed by chilling on ice and centrifuging for 10 s. To this, 5 μl of the 10× G7 reaction buffer [50 mM sodium phosphate (pH 7.5) at 25°C], 5 μl of 10% NP-40, 15 μl of water, and 5 μl of the deglycosylation enzyme cocktail (a mixture of glycerol-free PNGase F, *O*-glycosidase, neuraminidase, β1–4 galactosidase, β-*N*-acetylglucosaminidase) were added. The reaction mixture was incubated at 37°C overnight. The molecular mass of Slit in the treated sample was determined and compared to the nontreated sample as well as to the Slit in *mmy* mutant embryos by 4 to 12% SDS-PAGE. For PNGase F treatment, wild-type and mmy^{slm} embryos were collected and aged until 12–14 hpf. Protein extracts from about 40 embryos were prepared as above. For the reaction, 9 μl of the supernatant was mixed with 1 μl of the 10× glycoprotein denaturing buffer and incubated in boiling water bath for 10 min. To this, 2 μl of 10× G7 reaction buffer, 2 μl of 10% NP-40, 5 μl of water, and 1 μl of PNGase F were added. The reaction mixture was incubated at 37°C for 1 hour. After incubation, the protein sample was prepared for Western blotting by diluting with 10 μl of 4× Laemelli sample buffer, boiled in water for 10 min, and cooled on ice. For the untreated controls, the extracted protein sample was diluted with 10 μl of 4× Laemelli sample buffer and incubated in boiling water bath for 10 min. Equal amounts of PNGase F–treated and nontreated samples were electrophoresed using a 4 to 12% SDS-PAGE gel and Western blot analysis. The molecular weight before and after treatment was determined on the basis of mobility shift.

Immunoprecipitation

Because Robo1 was about threefold less abundant in *mmy*^{slm} embryos than in wild-type embryos, we used 500 *mmy*^{slm} embryos and 200 wildtype embryos for each immunoprecipitation experiment. Embryos that were aged for 12 to 14 hpf were homogenized in 37.5 μl of ice-cold lysis buffer [50 mM Hepes (pH 7.2), 100 mM NaCl, 1 mM $MgCl_2$, 1 mM $CaCl_2$, and 1% NP-40]. The lysates were incubated on ice for 30 min and centrifuged at 15,000g for 30min at 4°C. Thirty microliters of the supernatant was used as starting material for each IP reaction using the Catch and Release v2.0 Reversible Immunoprecipitation System (#17500; Millipore) using the manufacturer's instructions. The columns were washed three times with 1× wash buffer (Millipore) at 2000g for 20 s, and the IP was done by adding the following to the columns in the following order: 435 μl of 1×wash buffer, 30 μl of cell lysate, 25 μl of the antibody recognizing Slit-C, and 10 μl of antibody capture affinity ligand. The columns were then incubated overnight at 4°C. The flow-through was collected, and the columns were washed three times with 1× wash buffer (2000g, 20 s) before elution in 60 μl of phosphate-buffered saline–based denaturing elution buffer (2000g, 20 s). The proteins were then resolved on 4 to 12% SDS-PAGE and immunoblotted and probed with an antibody recognizing Robo1 (1:40, mouse, 13C9; DHSB).

Analysis of secreted versus nonsecreted Slit in embryos

To determine whether Slit was secreted in *mmy* mutants, we modified the embryo culture protocol of Perrimon and colleagues (26). Instead of culturing the cells from dissociated embryos for a period of time, we determined the presence or absence of Slit within and outside of the embryonic cells immediately after dissociation. Briefly, about 75 wildtype or *mmy*^{slm} embryos were collected, aged for specified number of hpf, and transferred into 500 μl of M3 insect cell culture medium, and the embryos were dissociated using a Dounce homogenizer with a loose fitting pestle to minimize cell lysis. We used five strokes without twisting the pestle for dissociation. Cells readily dissociated in M3 medium, as confirmed by visualizing an aliquot of the homogenate under a microscope. The homogenates were transferred to 1.5-ml Eppendorf tube and centrifuged at 4000g for 5 min. The supernatant was collected into a Vivaspin 500 (Sartorius) concentrator with a molecular weight cutoff of 100 and centrifuged at 15,000g for 17 min. The resulting ~30 μl of medium was then subjected to Western blot analysis for Slit. The pellet in the Eppendorf tube was washed once by gently resuspending the cells in 500 μl ofM3 medium and microfuging at 4000g for 5 min and discarding the supernatant. The pellets were then lysed using the lysis buffer for Western blot analysis and subjected to Western blot analysis for Slit using the Slit-C antibody.

Real-time qPCR

Wild-type and *mmy*^{slm} embryos were collected and aged until 12–14 hpf. They were dechorionated in 50% bleach and washed with water. One-hundred fifty wild-type and 150 homozygous mutant embryos were selected under the microscope, and total RNA was extracted using the RNaqueous kit (Ambion). The resulting RNA extract was deoxyribonuclease-treated and quantified using NanoDrop Spectrophotometer (NanoDrop

Technologies) and analyzed on RNA Nanochip using Agilent 2100 Bioanalyzer (Agilent Technologies). cDNA was synthesized using 1 μg of total RNA in a 20-μl reaction using the TaqMan Reverse Transcription Reagents kit (ABI). Reaction conditions were as follows: 25°C, 10 min; 48°C, 30 min; and 95°C, 5 min. Primers were designed and synthesized by the Molecular Genomic Core facility at the UTMB. Real-time PCR was done using 1.0 μl of cDNA in a total volume of 20 μl using the FastStart Universal SYBR green Master Mix (#04913850001; Roche). RpL32 was used as endogenous control. All PCR assays were performed in the ABI Prism 7500 Sequence Detection System under the following conditions: 50°C, 2 min; 95°C, 10 min; 40 cycles of 95°C, 15 s; and 60°C, 1 min. Primers used for *robo1* were 5′-CAGCATTAGTCTTCGTTGGGC-3′ (forward) and 5′-AATCCAACCAGTTTGCAGATTC-3′ (reverse). The qPCR was carried out on three separate embryo collections and in triplicate for each collection.

Image analysis using the ImageJ software

To determine the distribution of Robo1 and Slit across the CNS, ImageJ analysis was done using the plot.profile function across the nerve cord in defined areas. The analysis was performed on images from multiple embryos, although those shown in figures correspond to the panels shown in the figures.

Supplementary Material

Refer to Web version on PubMed Central for supplementary material.

Acknowledgments

We thank the New England Biolabs for providing samples of glycosidase enzymes free of charge, DHSB for antibodies (Fas II and Slit-C monoclonal), the Goodman laboratory for slithypo lines, and the Bloomington Drosophila Stock Center for various fly stocks. We are grateful to C. Desplan, C. Doe, and J. Berndt for reading the manuscript and for providing valuable suggestions. C. Desplan also helped improve the writing of the manuscript. We also thank D. Mohan for technical support during revision.

Funding: This project was funded by the NIH (National Institute of Neurological Disorders and Stroke) to K.M.B. (grant number NS09136701).

References

1. Kidd T, Bland KS, Goodman CS. Slit is the midline repellent for the robo receptor in Drosophila. Cell. 1999; 96:785–794. [PubMed: 10102267]
2. Simpson JH, Bland KS, Fetter D, Goodman CS. Short-range and long-range guidance by Slit and its Robo receptors: A combinatorial code of Robo receptors controls lateral position. Cell. 2000; 103:1019–1032. [PubMed: 11163179]
3. Rajagopalan S, Vivancos V, Nicolas E, Dickson BJ. Selecting a longitudinal pathway: Robo receptors specify the lateral position of axons in the Drosophila CNS. Cell. 2000; 103:1033–1045. [PubMed: 11163180]
4. Bhat KM, Gaziova I, Krishnan S. Regulation of axon guidance by Slit and Netrin signaling in the Drosophila ventral nerve cord. Genetics. 2007; 176:2235–2246. [PubMed: 17565966]
5. Harris R, Sabatelli LM, Seeger MA. Guidance cues at the Drosophila CNS midline: Identification and characterization of two Drosophila Netrin/UNC-6 homologs. Neuron. 1996; 17:217–228. [PubMed: 8780646]

6. Kolodziej PA, Timpe LC, Mitchell KJ, Fried SR, Goodman CS, Jan LY, Jan YN. frazzled encodes a Drosophila member of the DCC immunoglobulin subfamily and is required for CNS and motor axon guidance. Cell. 1996; 87:197–204. [PubMed: 8861904]
7. Mitchell KJ, Doyle JL, Serfini T, Kennedy TE, Tessier-Lavigne M, Goodman CS, Dickson BJ. Genetic analysis of Netrin genes in Drosophila: Netrins guide CNS commissural axons and peripheral motor axons. Neuron. 1996; 17:203–215. [PubMed: 8780645]
8. Li H, Chen J, Wu W, Fagaly T, Zhou L, Yuan W, Dupuis S, Jiang ZH, Nash W, Gick C, Ornitz DM, Wu JY, Rao Y. Vertebrate slit, a secreted ligand for the transmembrane protein roundabout, is a repellent for olfactory bulb axons. Cell. 1996; 96:807–818.
9. Rothberg JM, Jacobs JR, Goodman CS, Artavanis-Tsakonas S. slit: An extracellular protein necessary for development of midline glia and commissural axon pathways contains both EGF and LRR domains. Genes Dev. 1990; 4:2169–2187. [PubMed: 2176636]
10. Kidd T, Russell C, Goodmann CS, Tear G. Dosage-sensitive and complementary functions of roundabout and commissureless control axon crossing of the CNS midline. Neuron. 1998; 20:25–33. [PubMed: 9459439]
11. Keleman K, Rajagopalan S, Cleppien D, Teis D, Paiha K, Huber LA, Technau GM, Dickson BJ. Comm sorts Robo to control axon guidance at the Drosophila midline. Cell. 2002; 110:415–427. [PubMed: 12202032]
12. Eldar A, Dorfman R, Weiss D, Ashe H, Shilo BZ, Barkai N. Robustness of the BMP morphogen gradient in Drosophila embryonic patterning. Nature. 2002; 419:304–308. [PubMed: 12239569]
13. Nüsslein-Volhard C, Wieschaus E, Kluding H. Mutations affecting the pattern of the larval cuticle in Drosophila melanogaster. I. Zygotic loci on the second chromosome. Wilhelm Roux Arch Dev Biol. 1984; 193:267–282.
14. Araújo SJ, Aslam H, Tear G, Casanova J. mummy/cystic encodes an enzyme required for chitin and glycan synthesis, involved in trachea, embryonic cuticle and CNS development—Analysis of its role in Drosophila tracheal morphogenesis. Dev Biol. 2005; 288:179–193. [PubMed: 16277981]
15. Schimmelpfeng K, Strunk M, Stork T, Klämbt C. mummy encodes an UDP-N-acetylglucosamine-dipohosphorylase and is required during Drosophila dorsal closure and nervous system development. Mech Dev. 2006; 123:487–499. [PubMed: 16793242]
16. Mio T, Yabe T, Arisawa M, Yamada-Okabe H. The eukaryotic UDP-N-acetyl-glucosamine pyrophosphorylases, Gene cloning, protein expression, and catalytic mechanism. J Biol Chem. 1998; 273:14392–14397. [PubMed: 9603950]
17. Stanley P. Glycosylation engineering. Glycobiology. 1992; 2:99–107. [PubMed: 1606361]
18. Rini, J., Esko, J., Varki, A. Glycosyltransferases and glycan-processing enzymes. In: Varki, A.Cummings, RD.Esko, JD.Freeze, HH.Stanley, P.Bertozzi, CR.Hart, GW., Etzler, ME., editors. Essentials of Glycobiology. Vol. 2. Cold Spring Harbor: 2009. p. 63-73.
19. Altschul SF, Madden TL, Schäffer AA, Zhang J, Zhang Z, Miller W, Lipman DJ. Gapped BLAST and PSI-BLAST: A new generation of protein database search programs. Nucleic Acids Res. 1997; 25:3389–3402. [PubMed: 9254694]
20. Tonning A, Helms S, Schwarz H, Uv AE, Moussian B. Hormonal regulation of mummy is needed for apical extracellular matrix formation and epithelial morphogenesis in Drosophila. Development. 2006; 133:331–341. [PubMed: 16368930]
21. Brückner K, Perez L, Clausen H, Cohen S. Glycosyltransferase activity of Fringe modulates Notch-Delta interactions. Nature. 2000; 406:411–415. [PubMed: 10935637]
22. Moloney DJ, Panin VM, Johnston SH, Chen J, Shao L, Wilson R, Wang Y, Stanley P, Irvine KD, Haltiwanger RS, Vogt TF. Fringe is a glycosyltransferase that modifies Notch. Nature. 2000; 406:369–375. [PubMed: 10935626]
23. Okajima T, Xu A, Irvine KD. Modulation of notch-ligand binding by protein O-fucosyltransferase 1 and Fringe. J Biol Chem. 2003; 278:42340–42345. [PubMed: 12909620]
24. Doherty P, Cohen J, Walsh FS. Neurite outgrowth in response to transfected N-CAM changes during development and is modulated by polysialic acid. Neuron. 1990; 5:209–219. [PubMed: 2200449]

25. Manavalan MA, Gaziova I, Bhat KM. The midline protein regulates axon guidance by blocking reiteration of neuroblast rows within the ventral nerve cord. PLOS Gen. 2013; 9:e1004050.
26. Perrimon N, Zirin J, Bai J. Primary cell cultures from Drosophila gastrula embryos. J Vis Exp. 2011; 48:e2215.
27. Simpson JH, Kidd T, Bland KS, Goodman CS. Short-range and long-range guidance by Slit and its Robo receptors: Robo and Robo2 play distinct roles in midline guidance. Neuron. 2000; 28:753–766. [PubMed: 11163264]
28. Lee JS, Chien CB. When sugars guide axons: Insights from heparan sulphate proteoglycan mutants. Nat Rev Genet. 2004; 5:923–935. [PubMed: 15573124]
29. Johnson KG, Ghose A, Epstein E, Lincecum J, O'Connor MB, Van Vactor D. Axonal heparan sulfate proteoglycans regulate the distribution and efficiency of the repellent Slit during midline axon guidance. Curr Biol. 2004; 14:499–504. [PubMed: 15043815]
30. Bülow H, Hobert O. The molecular diversity of glycosaminoglycans shapes animal development. Annu Rev Cell Dev Biol. 2004; 22:375–407.
31. Lee JS, von der Hardt S, Rusch MA, Stringer SE, Stickney HL, Tallbot WS, Geisler R, Nüsslein-Volhard C, Selleck SB, Chien CB, Roehl H. Axon sorting in the optic tract requires HSPG synthesis by ext2 (dackel) and extl3 (boxer). Neuron. 2004; 44:947–960. [PubMed: 15603738]
32. Nybakken K, Perrimon N. Heparan sulfate proteoglycan modulation of developmental signaling in Drosophila. Biochim Biophys Acta. 2002; 157:280–291.
33. Steigemann P, Molitor A, Fellert S, Jäckle H, Vorbrüggen G. Heparan sulfate proteoglycan syndecan promotes axonal and myotube guidance by Slit/Robo signaling. Curr Biol. 2004; 14:225–230. [PubMed: 14761655]
34. Seiradake E, von Philipsborn AC, Henry M, Fritz M, Lortat-Jacob H, Jamin M, Hemrika W, Bastmeyer M, Cusack S, McCarthy A. Structure and functional relevance of the Slit2 homodimerization domain. EMBO Rep. 2009; 10:736–741. [PubMed: 19498462]
35. Roberts, DB. Drosophila: A Practical Approach. IRL Press; 1998.
36. Brand AH, Perrimon N. Targeted gene expression as a means of altering cell fates and generating dominant phenotypes. Development. 1993; 118:401–415. [PubMed: 8223268]
37. Bhat KM. Notch signaling acts before cell division to promote asymmetric cleavage and cell fate of neural precursor cells. Sci Signal. 2014; 7:ra101. [PubMed: 25336614]

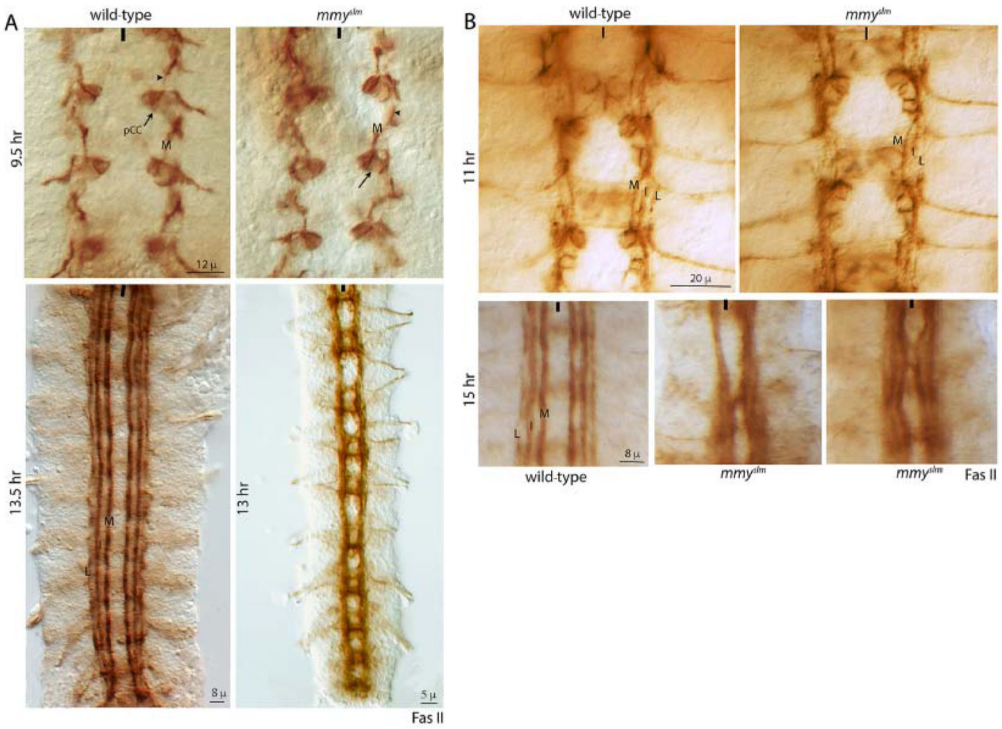

Figure 1. Loss of Mmy causes defects in axon guidance and tract positioning during the latter part of embryogenesis

CNS of embryos stained to show the neuronal marker Fas II. The anterior end is up, and the midline is marked by vertical lines at the top and bottom of each image. (**A**) Normal pCC neuron (arrow) that pioneers the M tract with its axonal projection (arrowhead) in wild-type and *mmy*^{slm} embryos at 9.5 hpf. Scale bar, 12 µm. (**B**) The M, I, and L tracts in wild-type and *mmy*^{slm} embryos at 11 hpf. Scale bar, 20 µm. (**C**) M, I, and L tracts in wild-type and *mmy*^{slm} embryos at 13.5, 13, and 15 hpf. Scale bars, 8 µm (top left), 5 µm (top right), 8 µm (bottom left), 15 µm (bottom middle), and 15 µm (bottom right). N > 10 independent experiments; n > 30 embryos per experiment.

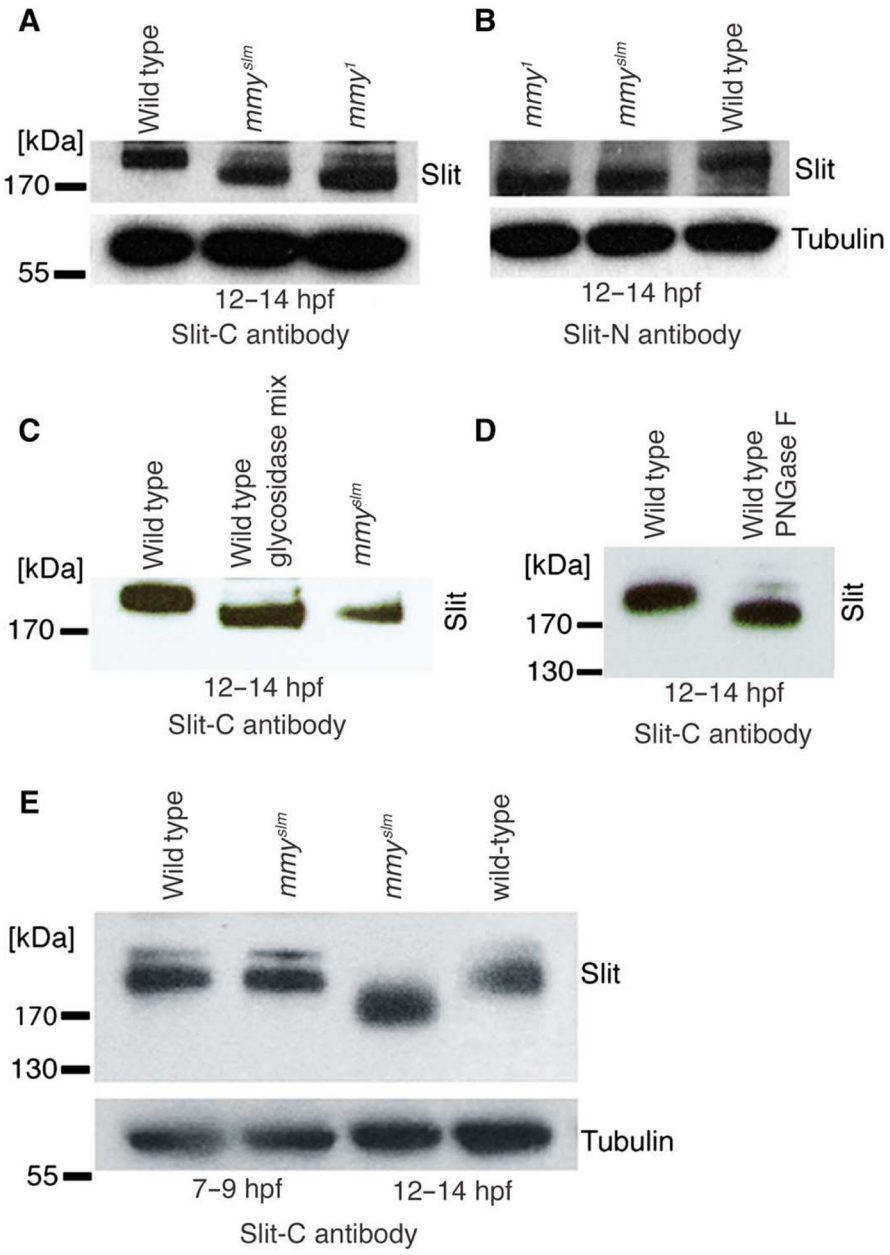

Figure 2. Mmy is required for the glycosylation of Slit

(**A** and **B**) Western blot analysis of extracts from 12- to 14-hpf wild-type, *mmy*^{slm}, and *mmy*^{1} embryos with antibodies recognizing Slit-C (A) and Slit-N (B). Only the full-length Slit is shown. Tubulin was used as loading control. $n > 3$ independent experiments. (**C**) Western blot analysis of Slit in extracts from 12- to 14-hpf wild-type embryos that were either untreated or treated with a glycosidase cocktail and from 12- to 14-hpf *mmy*^{slm} embryos. $n = 3$ independent experiments. (**D**) Western blot analysis of Slit in extracts from 12- to 14-hpf wild-type embryos that were either untreated or treated with the *N*-linked glycosidase PNGase F. $n = 2$ independent experiments. (**E**) Western blot analysis of Slit in

extracts from wild-type and *mmy*^{slm} embryos at 7 to 9 and 12 to 14 hpf, respectively. $N = 2$ independent experiments. The Slit-C antibody was used for the Western blots in (C) to (E).

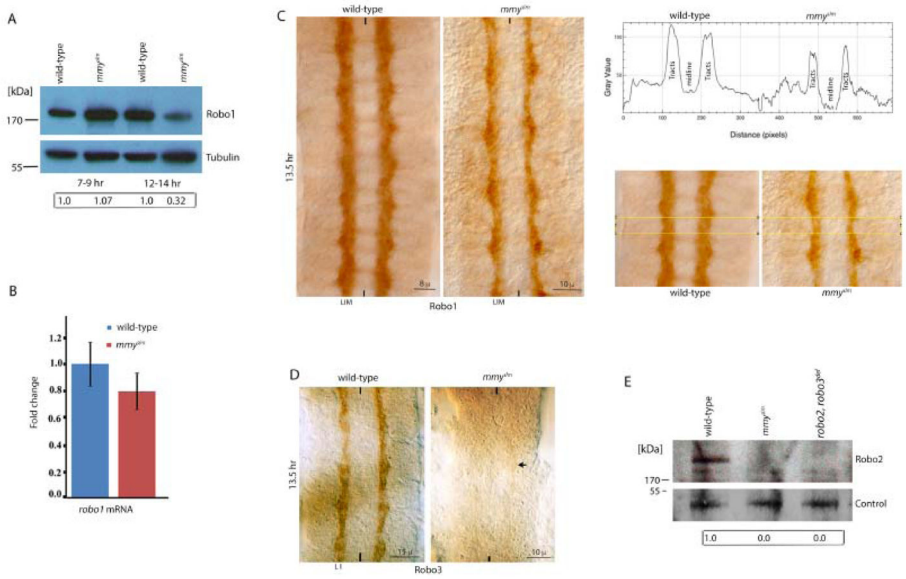

Figure 3. Loss of Mmy affects the abundance and distribution of Robo1, Robo2, and Robo3

(**A**) Western blot analysis of extracts from wild-type and *mmy*^{slm} embryos from two different developmental intervals with an antibody recognizing Robo1. The boxed numerical values with SD below the blot indicates the relative amounts of the Robo1 protein relative to wild type calculated from three independent experiments. The difference between wild type and the mutant was not statistically significant at 7 to 9 hpf ($P < 0.001$, Student's t test), whereas the difference was statistically significant at 12 to 14 hpf ($P < 0.001$, Student's t test). (B) qPCR analysis of robo1 expression in 12- to 14-hpf wild-type and *mmy*^{slm} embryos. The difference was not statistically significant ($P < 0.001$, Student's t test). (C) Robo1 in wildtype and *mmy*^{slm} embryos (left) and the distribution of Robo1 across the nerve cord as measured using the ImageJ software (right). The boxed areas in the images below the plot show the regions that were used for ImageJ analysis. (D) Robo3 in wild-type and *mmy*^{slm} embryos. The arrow indicates weak Robo3 staining in *mmy*^{slm}. (E) Western blot analysis of Robo2 in protein extracts from 12- to 14-hpf wild-type and *mmy*^{slm} embryos. The internal nonspecific band recognized by the antibody was used as a loading control. $N = 3$ (Western blotting and qPCR); $N = 3$ independent experiments; $n = 30$ to 60 embryos per experiment (immunohistochemistry); $n = 6$ embryos (ImageJ analysis). Scale bars, 8 μm.

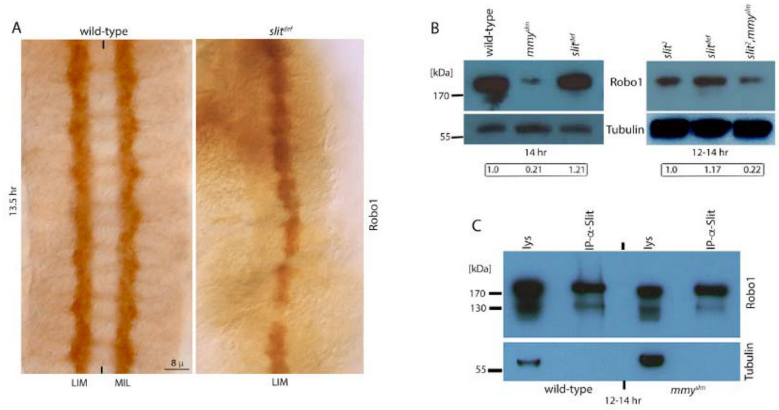

Figure 4. Reduction in the abundance of Robo1 in mmy is independent of Slit, and nonglycosylated Slit can bind to Robo1

(**A**) Robo1 in wild-type embryos and embryos homozygous for a deletion that removes slit (*slit*^{def}). $N > 6$ experiments; $n \geq 30$ embryos per experiment. Scale bar, 8 µm. (**B**) Western blot analysis of extracts from wild-type, *mmy*^{slm}, *slit*^{def}, *slit*^{2}, and *slit*^{2} *mmy*^{slm} double-mutant embryos. The boxed numerical values with SD below the blots indicate the relative amounts of Robo1 relative to wild type (left) or *slit*^{2} (right) calculated from three different experiments. The differences between wild type and *mmy*^{slm}, between *mmy*^{slm} and *slit*^{def}, and between *slit*^{2} or *slit*^{def} and *slit*^{2} *mmy*^{slm} double mutants were statistically significant ($P < 0.001$, Student's t test). (**C**) Western blot analysis of Robo1 in the lysates and Slit immunoprecipitates (IP-α–Slit-C) of extracts from 12- to 14-hpf wildtype, *mmy*^{slm}, and *slit*^{def} embryos. Tubulin was used as loading control; $N = 2$ independent experiments.

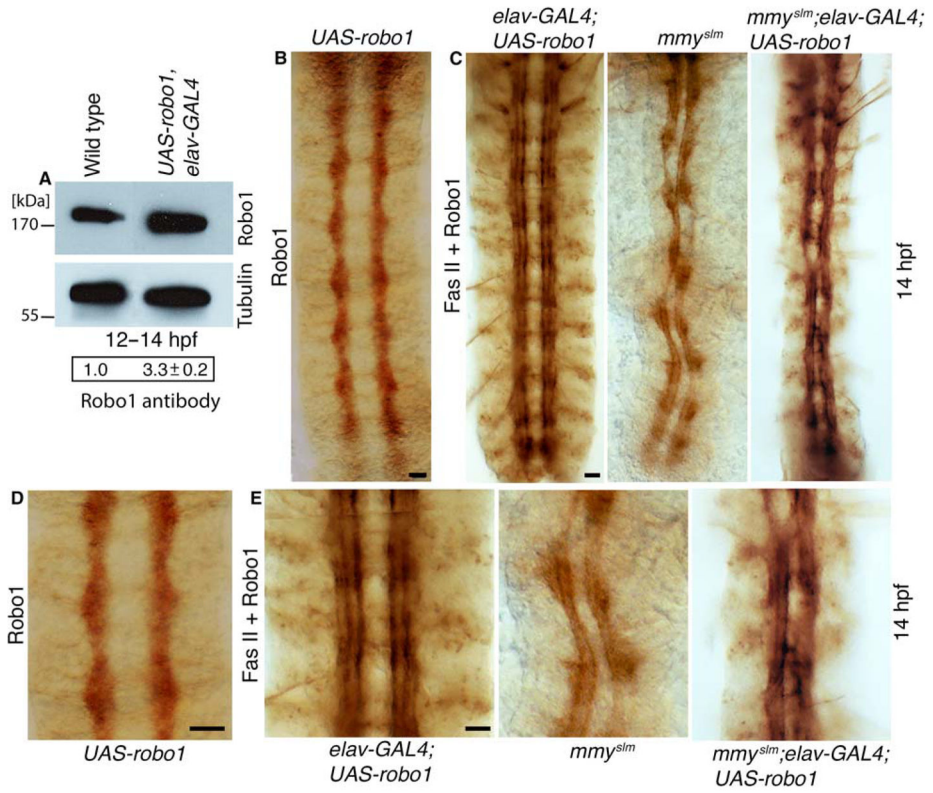

Figure 5. Pan-neuronal expression of robo1 does not rescue axon guidance defects in mmy mutants

(**A**) Western blot analysis of Robo1 in extracts from wild-type embryos and *UAS-robo1; elav-GAL4* embryos ectopically expressing robo1 in all neurons. The numerical values below the blot indicate the relative amounts of the Robo1 protein normalized to wild type. n = 3 experiments. The difference between the two was statistically significant ($P < 0.001$, Student's t test). (**B**) Robo1 exhibits wild-type distribution in *UAS-robo1* embryos not carrying a GAL4 driver. (**C**) Fas II (darker, discrete axon tracts staining) and Robo1 (lighter diffuse staining) in *UAS-robo1; elav-GAL4*, *mmy*^{slm}, and *mmyslm; elav-GAL4; UAS-robo1* embryos. Scale bar, 8 mm. (**D**) Magnified views of the CNS from embryos in (B) and (C). Scale bar, 4 μm. $N > 3$ experiments; $n \geq 60$ embryos per experiment.

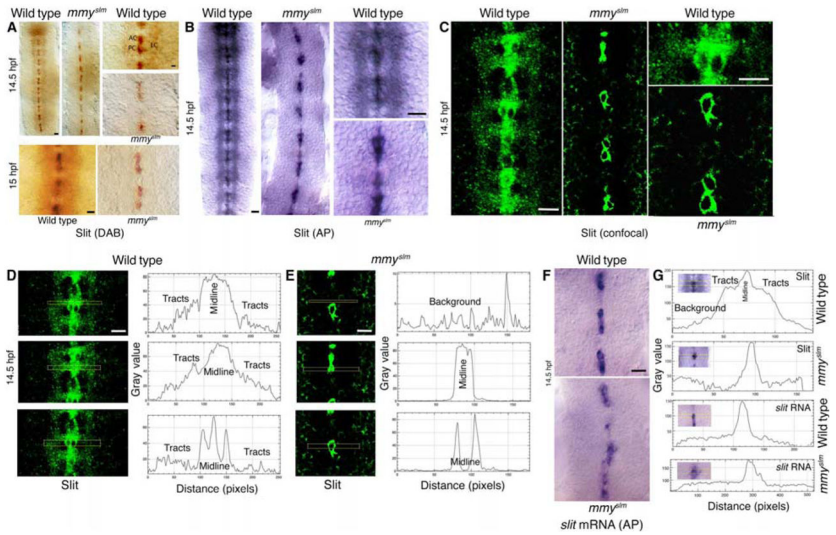

Figure 6. Glycosylation of Slit by Mmy is essential for the secretion of Slit from the midline cells

(**A** to **C**)Wild-type and *mmy*^{slm} embryos were immunostained with an antibody recognizing Slit-C and detected using secondary antibodies conjugated to DAB (A), AP (**B**), or a fluorescent tag (C). AC, anterior commissure; PC, posterior commissure; LC, longitudinal connectives. Confocal images were collected using the same microscope settings for both the wild type and the mutant. Scale bars, 8 μm (top left), 2.5 μm (top right), 4 μm (bottom) (A); 8 μm (B); and 4 μm (C). $N > 10$ experiments and $n > 60$ embryos per experiment (DAB and AP); $N = 2$ experiments and n > 30 embryos per experiment (fluorescence). (**D** and **E**) Distribution of the Slit protein across the nerve cord in wild-type and mmyslm embryos by ImageJ analysis. n ≥ 6 embryos. Scale bars, 4 μm. (**F**) *slit* RNA in wild-type and *mmy*^{slm} embryos showing slit expression in the midline cells. Scale bar, 5 μm. (**G**) Distribution of the Slit protein and *slit* mRNA across the nerve cord in wild-type and *mmy*^{slm} embryos by ImageJ analysis. $N \geq 2$ experiments; $n > 40$ embryos per experiment.

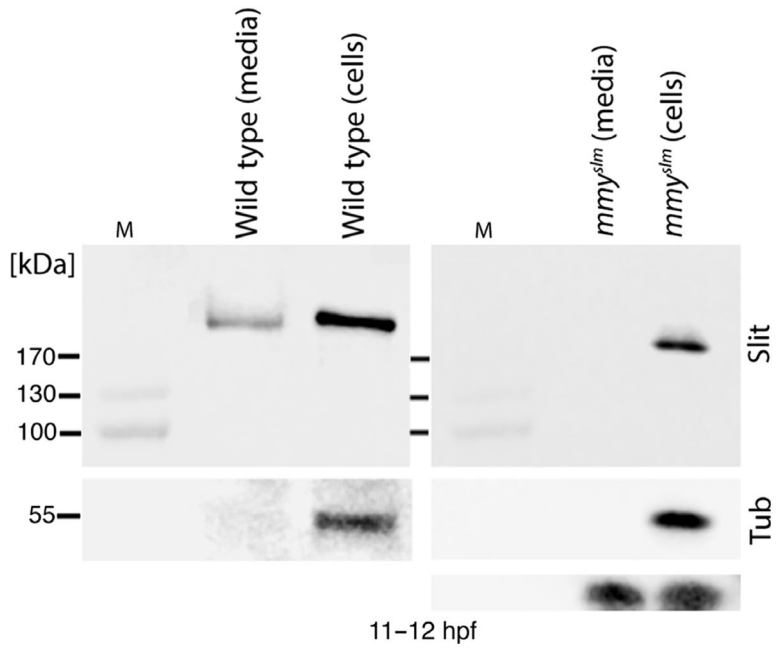

Figure 7. Slit is not secreted in mmy mutant embryos

Western blot analysis of the medium and cells of dissociated 11- to 12-hpf wild-type and *mmy*^{slm} embryos using an antibody recognizing Slit-C. $n > 3$ experiments. Tubulin (Tub) was used as a loading control and indicator of cell lysis. The Slit antibody cross-reacted with a band at <4 kDa in both the medium and the dissociated cells from *mmy*^{slm} embryos. M, molecular weight markers.

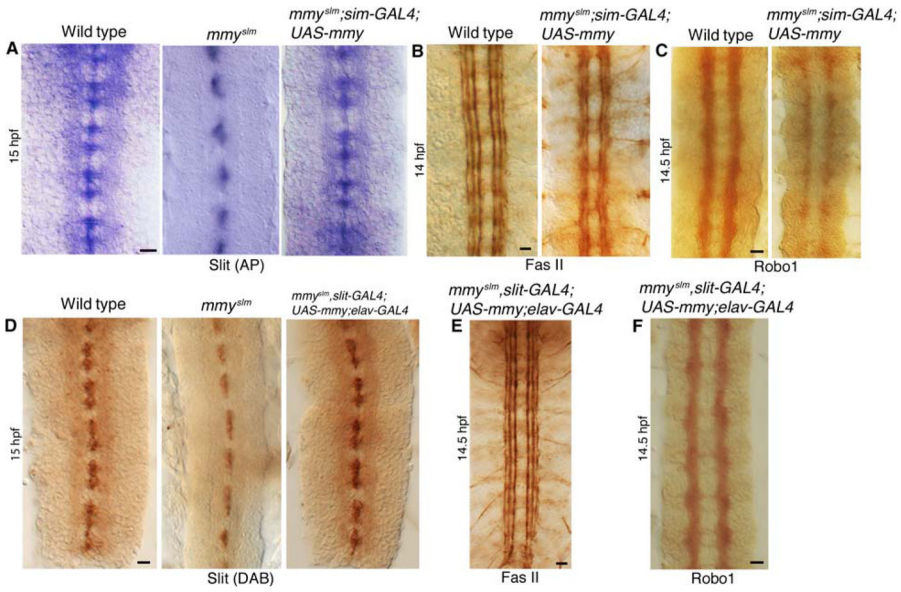

Figure 8. Expression of mmy in the midline cells rescues Slit secretion, loss of Robo1, and axon guidance defects in mmy mutants

(A to C) Rescue experiments in which a *UAS-mmy* transgene was expressed under the control of the midline driver *sim-GAL4*. (A) Distribution of Slit, as detected by AP reaction, in wild-type, mmy^{slm}, and mmy^{slm}; *sim-GAL4; UAS-mmy* embryos. $n = 2$ experiments; $n = 20$ embryos per experiment. (B) Fas II staining of axon tracts in wild-type and mmy^{slm}; *sim-Gal4; UAS-mmy* embryos. $N = 3$ experiments; $n = 30$ embryos per experiment. (C) Distribution of Robo1 in the axon tracts in wild-type and mmy^{slm}; *sim-GAL4; UAS-mmy* embryos. $n = 3$ experiments; $n = 30$ embryos per experiment. (D to F) Rescue experiments in which a *UAS-mmy* transgene was expressed under the control of the midline driver *slit-GAL4* and the pan-neuronal driver *elav-GAL4*. (D) Slit distribution in wild-type, mmy^{slm}, and mmy^{slm}, *slit-GAL4; UAS-mmy; elav-GAL4* embryos. $N = 2$ experiments; $n = 20$ embryos per experiment. (E) Fas II staining of the axon tracts in mmy^{slm}, *slit-GAL4; UAS-mmy; elav-GAL4* embryos. $N = 3$ experiments; $n = 30$ embryos per experiment. (F) Distribution of Robo1 in mmy^{slm}, *slit-GAL4; UAS-mmy; elav-GAL4* embryos. $N = 2$ experiments; $n = 20$ embryos per experiment. Scale bars, 8 μm.

Table 1

Distance between the axon tracts and thickness of the tracts in wild-type and *mmy*^{slm} embryos

Measurement of the distance between axon tracts across the midline (in micrometers with SD) and the thickness of the tracts. Each measurement represents the mean from three to six different embryos for each time point. I and L are not yet present in the 9.5-hpf embryos. M-M is the distance between the left and right M tracts across the midline, L-L is the distance between the left and right L tracts, and I-I is the distance between the left and right I tracts. The difference in the distance between tracts in wild-type and *mmy*^{slm} mutant embryos was statistically significant only at 14 hpf ($P < 0.001$, two-tailed P value using the Student's t test). The distance between tracts is given as a range for *mmy*^{slm} embryos at 14 hpf because of the guidance defects. ND, not determined due to severe axon positioning defects.

Age			9.5 hpf		11.0 hpf		14.0 hpf	
Genotype			Wild type	*mmy*^{slm}	wild type	*mmy*^{slm}	Wild type	*mmy*^{slm}
Tracts (Fas II)	Distance between (μm)	M-M	23.3 ± 0.4	24.1 ± 0.3	20.8 ± 0.4	20.7 ± 0.3	8.1 ± 0.1	2.6 ± 0.2 to 5.1 ± 0.3
		I-I	—	—	24.4 ± 0.4	24.5 ± 0.4	16.3 ± 0.3	5.9 ± 0.4 to 11 ± 0.5
		L-L	—	—	28.5 ± 0.5	28.5 ± 0.4	27.4 ± 0.5	9.3 ± 0.5 to 18.7 ± 0.8
	Thickness (μm)	M or I	0.7	0.7	0.7–0.8	0.7–0.8	2.0	1.0 to 2.0
		L	—	—	0.4	0.4	0.8	ND

Table 2

Distance between and thickness of the tracts in wild-type and *mmy*^{slm} rescue embryos

The distance between axon tracts across the midline (in micrometers with SD) and the thickness of the tracts in two different rescue experiments. The values given are as a mean with SD compiled from six different embryos. M-M is the distance between the left and right M tracts across the midline, L-L is the distance between the left and right L tracts, and I-I is the distance between the left and right I tracts. There was no significant difference between wild-type embryos and *mmy*^{slm} mutants expressing a *mmy* transgene in midline cells and pan-neuronally (*mmy*^{slm}, *slit-GAL4; UAS-mmy;elav-GAL4*). $P < 0.001$, two-tailed P value using the Student's t test. There was a statistically significant difference between wild-type embryos and *mmy*^{slm} mutants expressing a *mmy* transgene in midline cells only (*mmy*^{slm}, *sim-GAL4;UAS-mmy*). $P < 0.001$, Student's t test. ND, not determined.

Age			**14.5 hpf**		
Genotype			**Wild type**	***mmy*^{slm}, *sim-GAL4;UAS-mmy***	***mmy*^{slm}, *slit-GAL4; UAS-mmy;elav-GAL4***
Tracts (Fas II)	Distance between (μm)	M-M	8.0 ± 0.1	5.0 ± 0.1 to 7.5 ± 0.1	8.0 ± 0.1 to 9.0 ± 0.1
		I-I	16.8 ± 0.2	ND	17.0 ± 0.2
		L-L	27.0 ± 0.5	22.0 ± 0.4	28.0 ± 0.4
	Thickness (μm)	M or I	2.0	1.6	2.0
		L	0.8	0.8	0.8

Sci Signal. Author manuscript; available in PMC 2018 March 12.